A Low-Cost Bioimpedance Phase Angle Monitor for Portable Electrical Surface Stimulation Burn Prevention

Ryan P. Burns, Jeremy Dunning, *Member, IEEE,* and Michael J. Fu, *Member, IEEE*

***Abstract*— Electrical skin-surface stimulation has wide clinical adoption and home use, but skin burns are a risk and existing devices do not monitor the electrode sites for skin damage or improperly connected electrodes. When a burn occurs, the low frequency phase of the skin surface impedance changes. This paper describes a novel analog processing technique that is suitable for detecting skin surface phase changes during the use of portable electrical stimulation devices. The output is a 1-bit signal indicating if the phase has changed by more than a predetermined amount, allowing the system to be incorporated into low-cost devices with limited processing capability. Computational simulations were performed using a current-sourced bipolar square-wave stimulation signal. An approximation is presented which converts a phase change in the skin-surface impedance to a voltage, which was found to have an average error of 14.1%. Due to the analog techniques used, there is a propagation delay of 232.48 ms between the phase exceeding the allowable threshold and the output being set to HIGH. These initial simulation results provide evidence for the feasibility of developing safer portable skin surface electrical stimulators that can monitor and prevent skin injury during clinical or home use.**

***Index Terms*—analog signal processing, bioimpedance, biomedical monitoring, burn, phase, skin surface stimulation.**

I. Introduction

ELECTRICAL surface stimulation (ESS) is a stimulation technique used in a wide variety of clinical applications, including but not limited to: diagnosis of medical conditions, muscle strengthening, injury recovery [1], and pain reduction [2]. To apply this stimulation, the majority of techniques use surface electrodes, but burns and rashes at the electrode sites are possible risks [2]. Multiple mechanisms have been proposed to explain the source of these burns such as high current density and high pH changes [2]-[3]. Stecker et al. focuses on joule heating, in which burns are the result of an increase in the temperature of the skin due to electrical current [4]. According to Stecker et al., burns due to constant-current, bipolar stimulation are dependent on electrode-skin contact area, tissue conductivity, magnitude of the current, and time exposed (typically occurring over the course of multiple seconds under burn-inducing conditions [4]).

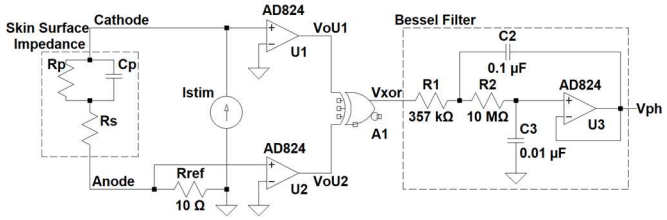

Fig. 1. The Phase-Voltage Converter schematic, in which R_S, R_P, and C_P are used to model the skin surface impedance, and V_{ph} is the output.

The skin-surface impedance (SSI) model proposed in the literature (Fig. 1), is an RC circuit comprised of R_S, C_P, and R_P, though if modeling the more complex properties of the SSI, R_p would be time-varying and non-linear [5]. Patriciu et al. found that when skin was burned by electrical surface stimulation, the low frequency spectrum of the SSI changed drastically due to the breakdown of C_p, showing that a change in the phase of the SSI may indicate the onset of a burn [3].

Yu et al. proposed a bioimpedance measuring system that uses digital signal processing to determine both the magnitude and phase of the impedance at the stimulation frequency [6]. The phase shift of a single frequency, sinusoidal voltage across a complex impedance is linearly proportional to the phase of the impedance, and as such the phase of the bioimpedance can be determined by monitoring the time shift of the voltage. Figure 1 shows a modified version of the analog front end of the system proposed by Yu et al. [6], which is used in the current system. Yu et al.'s system requires data acquisition and computational hardware that can increase the size and cost of an otherwise portable stimulation device. Moreover, it cannot continuously monitor the phase of the impedance during stimulation that involves square-wave stimulation due to the infinite odd harmonics introducing a non-linear and non-trivial time shift.

Portable, low-cost methods for preventing skin injury during clinical ESS do not exist and are needed. Clinical devices have power, space, and processing constraints that preclude the feasibility of algorithms that require extensive error correction

This paper was submitted for review on August 18, 2020. This work was supported in part by the National Science Foundation grant CBET 1942402.

R. P. Burns (rpb83@case.edu) and M. J. Fu (mjf24@case.edu) are with the Dept. of Electrical, Computer, and Systems Engineering of Case Western Reserve University, Cleveland, OH 44124 USA. J. Dunning is with the Advanced Platform Technologies Center and M. J. Fu is with the Cleveland Functional Electrical Stimulation Center, both of which are at the Louis Stokes Cleveland Dept. of Veterans Affairs Medical Center, Cleveland, OH 44106. M. J. Fu is also with MetroHealth Rehabilitation Institute, MetroHealth System, Cleveland, OH 44109

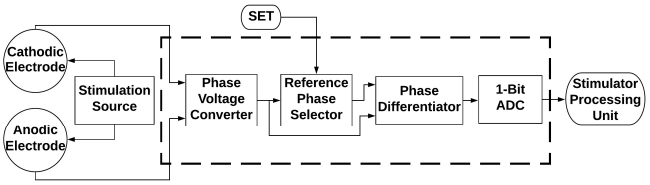

Fig. 2. A block diagram for the proposed Bioimpedance Phase Angle Monitor. The dashed box contains the system proposed by this paper.

or signal processing, which are needed for bipolar, square-wave constant-current stimulation [7].

The current paper describes the design and simulation of a novel system that detects changes in the SSI in order to prevent burns during ESS when administered by devices using current-controlled, bipolar, square-wave stimulation. This system improves upon prior voltage-based impedance detection techniques [6] by eliminating the need for data acquisition and reducing processing burden to only 1 bit of data. Further, the current paper proposes a novel approximation of the time shift as a function of phase when a square-wave voltage (induced by a current source) is applied to a complex impedance.

II. System Design

The system (Fig. 2) initially behaves as a standard surface stimulator. The system has two analog inputs, a 1-bit digital input (SET), and a 1-bit digital output (B_0). When stimulation is applied at its desired frequency and phase, SET provides a logical HIGH pulse, which assigns the current phase of the SSI to the reference phase of the system. If, after SET has been triggered, the phase of the SSI changes by more than a predetermined amount, then the digital output of the system will be set to HIGH, indicating to the user that the electrodes may need to be reapplied or removed to inspect for skin irritation.

A. Phase-Voltage Converter

The Phase-Voltage Converter (Fig. 1) is based on the phase detection system described by Yu et al. [6]. The stimulation source is connected directly to the cathodic electrode, and connected to the anodic electrode through R_{ref}. The cathodic and anodic electrodes are the analog inputs to the system, and their respective voltages are measured by the comparators formed by U1 and U2. All op-amps in Fig. 1, and the entire system, are powered by single supply, resulting in an output of V_{dd} when the input to the comparators are positive, and zero volts when the inputs are negative. The XOR logic gate A1 gives an output, V_{XOR}, that is HIGH when either V_{Cathode} or V_{Anode} is positive, but not both (Fig. 3).

Figure 3 shows that the width of V_{XOR}'s pulse is equal to t_{d}, the time delay between the zero-crossing points of V_{Cathode} and V_{Anode}. V_{XOR} is then passed as an input to a 2nd order low pass Bessel filter. The filter is designed with a passband defined by the -3 dB point of 2 Hz in order to remove the higher frequency components from V_{XOR}. This results in V_{ph} equaling the DC average of V_{XOR}, which can be calculated as

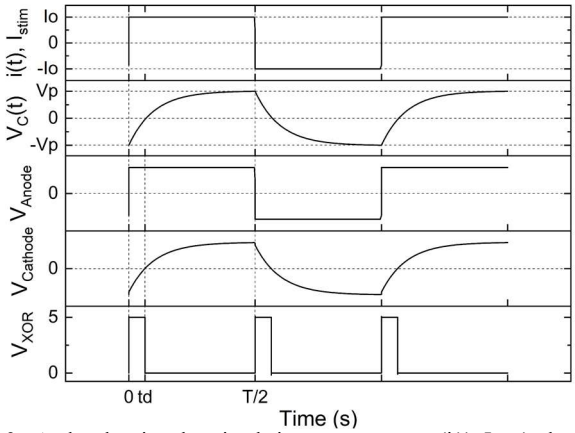

Fig. 3. A plot showing the stimulation current source (i(t), I_{STIM}), the voltage across C_{p} in Fig. 1 ($V_{\text{C}}(t)$), the voltage measured by U1 and U2 (V_{Cathode} and V_{Anode}, respectively), and the output of A1 in Fig. 1 (V_{XOR}).

$$V_{\text{ph}} = \frac{2V_{\text{dd}}t_{\text{d}}}{T}, \tag{1}$$

in which T is the period of the square wave.

Assuming steady state, Fig. 3 shows the expected voltage across C_{p} in Fig. 1, $V_{\text{c}}(t)$, when a square wave current with no DC offset is applied to the SSI model. $V_{\text{c}}(t)$ oscillates between $-V_{\text{p}}$ and V_{p}, while the stimulation source, $i(t)$, switches between $-I_0$ and I_0, as shown in Fig. 3.

The time delay, t_{d}, can be determined by focusing on the first half period of $i(t)$ in Fig. 3. At time $t = 0$, $i(t)$ goes from $-I_0$ to I_0, and at time $t = T/2$, $i(t)$ goes from I_0 to $-I_0$. $V_{\text{c}}(t)$ can be described by the first-order, linear differential equation,

$$C_{\text{p}}\dot{V}_{\text{c}} + \frac{1}{R_{\text{p}}}V_{\text{c}} = I_0. \tag{2}$$

Solving (2) for $t > 0$, and $V_{\text{c}}(0) = -V_{\text{p}}$, the voltage across the capacitor can be analytically described by

$$V_{\text{c}}(t) = \left(I_0R_{\text{p}} + V_{\text{p}}\right)\left(1 - e^{-\frac{t}{\tau}}\right) - V_{\text{p}}\,, \tag{3}$$

in which $\tau = R_{\text{p}}C_{\text{p}}$. V_{p} can then be solved for by setting $V_{\text{c}}\left(\frac{T}{2}\right)$ equal to V_{p}, resulting in

$$V_{\text{p}} = \frac{I_0R_{\text{p}}\left(1 - e^{-\frac{T}{2\tau}}\right)}{1 + e^{-\frac{T}{2\tau}}}. \tag{4}$$

The voltage across R_{s}, R_{p}, and C_{p} represents the potential across the skin surface, which can be found using (3) and (4) as

$$V_{\text{SSI}}(t) = V_{\text{c}}(t) + I_0R_{\text{s}} \tag{5}$$
$$= I_0\left(\left(1 - \frac{2e^{-\frac{t}{\tau}}}{1 + e^{-\frac{T}{2\tau}}}\right)R_{\text{p}} + R_{\text{s}}\right)$$

Since the current source has a zero-crossing point at $t = 0$, the time delay in the zero-crossing point is simply the time t_{d} such that $V_{\text{SSI}}(t_{\text{d}}) = 0$. Solving (5) for t_{d} results in

$$t_{\text{d}} = -\tau \ln\left(\frac{\left(1 + \frac{R_{\text{s}}}{R_{\text{p}}}\right)\left(1 + e^{-\frac{T}{2\tau}}\right)}{2}\right). \tag{6}$$

R_s, R_p, and C_p can be modeled as a single complex impedance, Z_{SSI}. Assuming for a moment that $i(t)$ is a sinusoid with period T and frequency $\omega = \frac{2\pi}{T}$, the reactance of C_p can be written as $\frac{1}{j\omega C_p}$. The series combination of R_s with the parallel combination of R_p and C_p results in $Z_{SSI} = R_s + \frac{R_p}{1+j\omega C_p R_p}$. Therefore, the phase of Z_{SSI} is

$$\varphi = \tan^{-1}\left(-\frac{\omega C_p R_p^2}{R_s + R_p + \omega^2 C_p^2 R_p^2 R_s}\right). \quad (7)$$

Although equation (6) gives the delay, it cannot be solved when line monitoring the phase of the SSI without digital processing because the distinction between R_s, R_p, and C_p will be unknown. References [5] and [8] experimentally found that $R_s \approx 350\ \Omega$, $C_p \approx 0.02\ \mu$F, and $R_p \approx 10 - 24\ k\Omega$. Therefore, (6) and (7) can be approximated by assuming that $R_p \gg R_s$.

$$t_d \approx -\tau \ln\left(\frac{1 + e^{-\frac{T}{2\tau}}}{2}\right) \quad (8)$$

$$\varphi \approx \tan^{-1}(-\omega C_p R_p) = \tan^{-1}(-\omega\tau) \quad (9)$$

Solving (9) for τ and plugging into (8) gives

$$t_d \approx \frac{T}{2\pi}\tan(\varphi)\ln\left(\frac{1 + e^{\frac{\pi}{\tan(\varphi)}}}{2}\right). \quad (10)$$

Combining (10) with (1), an approximation of V_{ph} as a function of SSI phase can be determined as

$$V_{ph} \approx \frac{V_{dd}}{\pi}\tan(\varphi)\ln\left(\frac{1 + e^{\frac{\pi}{\tan(\varphi)}}}{2}\right). \quad (11)$$

With this approximation, changes in the phase of the SSI should be reflected by changes in V_{ph}, which is easily monitored.

B. Reference Phase Selector

In order to set a reference voltage to compare V_{ph} against, a sample and hold (S&H) circuit is used, as shown in Fig. 4. U4 and U5 are used as high impedance buffers to reduce the discharging of the capacitor, C_4. The digital signal SET is used to control the S&H, with HIGH, or V_{dd}, setting V_{ref} to V_{ph}, and LOW, or 0 V, maintaining the current V_{ref}.

C. Phase Differentiator

The Phase Differentiator, shown in Fig. 4, monitors the changes in the phase of the SSI. This circuit has two inputs: V_{ph} (the current phase of the SSI) and V_{ref} (the reference phase of the SSI). U6 and U7 are set up as complimentary difference circuits, using standard op-amp topologies. The output of U6 is $3(V_{ph} - V_{ref})$ when $V_{ph} > V_{ref}$, and 0 otherwise. Conversely, the output of U7 is $3(V_{ref} - V_{ph})$ when $V_{ph} < V_{ref}$, and 0 otherwise.

The output of the Phase Differentiator, V_{dif}, is the average of the outputs of U6 and U7. Thus, for all V_{ph} and V_{ref}, V_{dif} can be described by

$$V_{dif} = \frac{3}{2}|V_{ph} - V_{ref}|. \quad (12)$$

As shown by (11), V_{ph} and V_{ref} can be approximated as a function of the phase of the surface impedance. Subsequently,

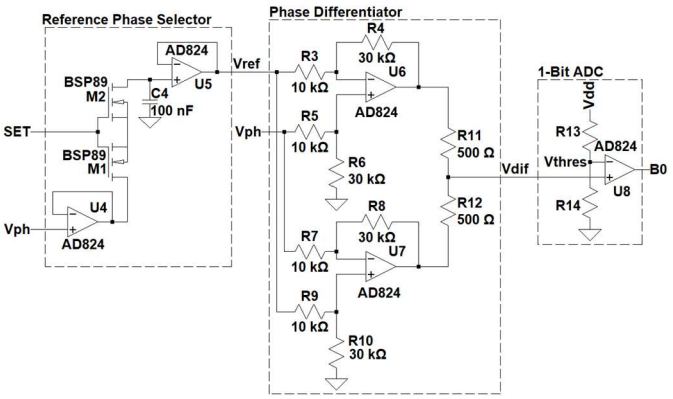

Fig. 4. The schematic for the Reference Phase Selector (inputs V_{ph} and SET, output V_{ref}), the phase differentiator (inputs V_{ref} and V_{ph}, output V_{dif}), and the 1-Bit ADC (input V_{dif}, output B_0).

V_{dif} can be approximated in terms of the reference phase and the instantaneous phase.

$$V_{dif} \approx \frac{3}{2}\frac{V_{dd}}{\pi}\left|\tan(\varphi)\ln\left(\frac{1 + e^{\frac{\pi}{\tan(\varphi)}}}{2}\right) - \tan(\varphi_{ref})\ln\left(\frac{1 + e^{\frac{\pi}{\tan(\varphi_{ref})}}}{2}\right)\right| \quad (13)$$

D. 1-Bit ADC

The differential voltage generated by the Phase Differentiator, V_{dif}, is then passed into the final stage of the system, the 1-Bit ADC. The ADC output, B_0, is HIGH when the differential voltage V_{dif} exceeds a predetermined voltage, V_{thres}. The proposed system uses a standard op-amp based comparator topology for the ADC, as shown in Fig. 4.

As is clear from (13), V_{dif} is not symmetric around φ_{ref}; hence, the selection of V_{thres} sets a maximum phase increase that is not equal to the maximum phase decrease. Therefore, V_{thres} cannot be set to an exact phase change. In addition, V_{dif} is dependent on φ_{ref}, the exact value of which will be unknown during the proposed implementation. As such, V_{thres} is chosen to correspond to an approximate maximum phase change.

III. Experiment

Simulations were run in LTSpice XVII and used Analog Devices' and Nexperia's spice models for the AD824 op-amp and the BSP89 transistor, respectively. The LTSpice behavioral XOR model, adjusted to the 74HC86 (Vhigh = 5 V; Trise = Tfall = 7 ns) [9], was used to model A1 in Fig. 1.

The simulations were performed assuming that in the SSI RC model used (Fig. 1), R_S is orders of magnitude lower than R_P. Further, it was assumed that R_P behaves as a linear, non-current dependent resistor, unlike the more advanced model presented by Dorgan and Reilly [5]. These assumptions were made in order to simplify the approximation of V_{dif}, as given by (13).

As shown by (13), V_{dif} is independent of the magnitude of the SSI and the frequency of the stimulation signal. To verify this independence, testing was performed at SSI magnitudes, when

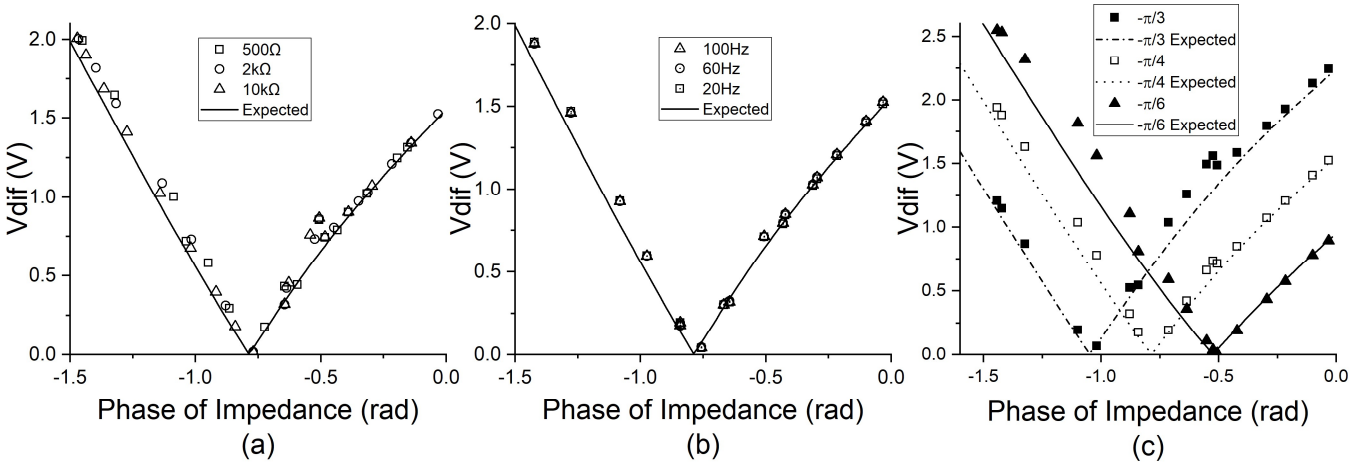

Fig. 5. V_{dif} versus the phase of the impedance over the range of anticipated conditions. Unless otherwise stated, tests were performed with SSI magnitude of 2 kΩ, reference phase of –π/4 rad, stimulation square wave frequency of 100 Hz and amplitude 100 mA. (a) Testing was performed over the range of anticipated SSI magnitudes (500, 2 k, and 10 kΩ). (b) Testing was performed over the range of anticipated frequencies (20, 60, and 100 Hz). (c) Testing was performed over a range of reference phases (-π/3, -π/4, and -π/6 rad).

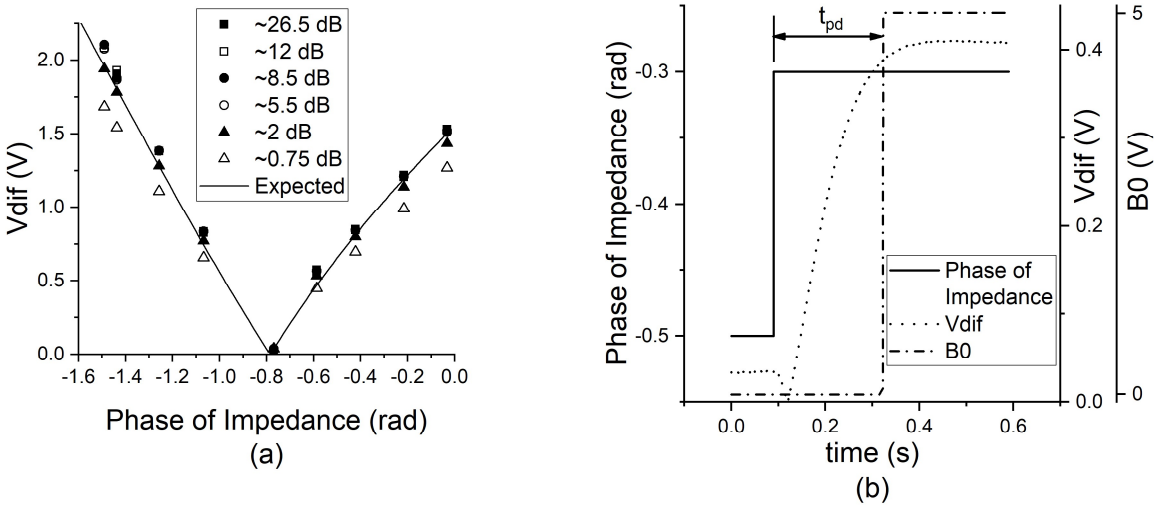

Fig. 6. (a) V_{dif} versus the phase of the SSI model over a range of stimulation SNR. These simulations used SSI magnitude of 2 kΩ and reference phase –π/4 rad, when evaluated at the stimulation frequency of 100 Hz. The stimulation signal had an amplitude of 100 mA. (b) Simulations were run with a reference phase of -0.5 rad, V_{thres} set to 0.388 V (which is a maximum phase increase from -0.5 rad of 0.2 rad), a stimulation frequency of 60 Hz, and SSI magnitude of 2 kΩ.

evaluated at the fundamental frequency of the stimulation signal, of 500, 2 k, and 10 kΩ, as per the standard set by the FDA for muscle stimulators in [10]. Further, the system was tested over the range of anticipated stimulation frequencies, 20 to 100 Hz, as per the Agency for Clinical Innovation [1].

The system was further tested by including Additive White Gaussian Noise (AWGN) in the stimulation signal. The AWGN was added by including a behavioral current source in parallel with the stimulation current source in the simulation. The behavioral current source was governed by the equation $I = \text{white}(1e5 * \text{time})/\{\text{Noise}\}$, in which {Noise} is a variable used to vary the power of the noise. The SNR of the stimulation signal was calculated using $\text{SNR}_{\text{stim}} = 20\log_{10}\frac{I_{\text{stim,RMS}}}{I_{\text{AWGN,RMS}}}$.

IV. Results

Figure 5 summarizes the simulations performed over the anticipated range of stimulation conditions. The magnitudes and phases of the SSI are as calculated at the fundamental frequency of the stimulation signal for the particular simulation. The average percent error between the simulated V_{dif} and the expected V_{dif}, as calculated by (13), for all simulations in Fig. 5 is 14.1%, with one outlier excluded. The outlier had $\varphi \approx \varphi_{\text{ref}}$ ($V_{\text{dif, expected}} = 0.195$ mV) with an absolute error of 33.99 mV, which corresponds to a percent error of 17,435%. 50.3% of values had an error of less than 7.82%. The simulations incorporating AWGN are summarized in Fig. 6a. The average error for tested stimulation SNRs between 2 and 26.5 dB were found to be between 30.7 and 72.7 mV. The average error was

found to be as high as 165 mV for a stimulation SNR of 0.75 dB. The delay between the change in phase and the rising edge of B_0 is shown in Fig. 6b, in which the reference phase is -0.5 rad, with V_{thres} set to 0.388 V, which equates to a maximum phase increase of 0.2 rad. The plot shows the settling of V_{dif} in response to an instantaneous phase change from -0.5 to -0.3 rad, and the delay in B_0, which is 232.48 ms. The delay was also found for a gradual increase from -0.5 to -0.3 rad (184 ms), and a gradual decrease from -0.5 to -0.7 rad (74 ms).

V. Discussion

The simulated system was found to indicate changes in the phase of an RC circuit, which models the SSI, within 14.1% of the expected value. This indicates that the system could be used to monitor phase changes in the SSI during ESS, without requiring data acquisition and computational hardware; however, the system has relatively large error when measuring an exact phase change due to the approximations made. Since variations in the phase of the SSI can indicate the onset of a burn or burn inducing conditions [3]-[4], the system could help decrease the likelihood of burns during ESS.

The delay of the system, at 232.48 ms, is dominated by the settling time of the Bessel filter, and as a result could be significantly reduced using digital processing and bypassing the filter entirely. The tradeoff of decreasing the delay by increasing processing is likely unnecessary as burns due to joule heating during ESS typically occur over the course of multiple seconds [4], which is longer than the simulated delay. In addition, the tradeoff would eliminate the primary advantage of the proposed system: the negligible required processing.

The simulated system improves upon the design by Yu et al. [6] by approximating the phase based off of constant-current, bipolar, square-wave stimulation, as opposed to a sinusoidal voltage signal, and can do so without data acquisition nor a microcontroller unit [6]. This allows the phase to be monitored during stimulation without modifying the delivered stimulation.

The error in V_{dif} is in part due to the discharging of C_4 in the S&H circuit. This decreases the reference voltage and can lead to an inaccurately high V_{dif}. As such, the proposed system could likely be improved by a more robust reference phase selector.

Many of the system's limitations are due to the analog techniques presented. By digitizing the signal immediately after the XOR gate, the delay due to the filter and the error due to the discharge of the S&H could be eliminated. The disadvantages of digitization is that it requires significantly more processing and digital I/Os than the analog technique presented, which may not be available in pre-existing, portable stimulators.

VI. Conclusion

A novel circuit was developed to detect changes in the low frequency phase of the skin surface impedance during portable electrical skin-surface stimulation, specifically for constant-current, bipolar square-wave stimulation with no DC-offset. The system, as proposed, requires few components, few inputs, and negligible digital processing to interpret the output. The system can effectively indicate when a maximum allowable phase change is exceeded. If incorporated into surface stimulators, the proposed circuit could help indicate the onset of a burn or even prevent burns altogether without delivering additional signals to the surface electrodes nor pausing the stimulation to measure the impedance. Although our system has higher phase estimation error and propagation delay relative to digital systems, its performance was found to be suitable for skin injury prevention during ESS and its design was consistent with our prioritization of low-cost clinical viability. Further work is warranted, and includes the physical implementation of the proposed circuit, human trials of the detector, and digitizing the signal instead of the proposed analog processing.

References

[1] "Using-Electrical-Stimulation-January-2014.pdf." Accessed: May 18, 2020. [Online]. Available: https://www.aci.health.nsw.gov.au/__data/assets/pdf_file/0004/211819/Using-Electrical-Stimulation-January-2014.pdf.

[2] A. Patriciu, K. Yoshida, J. J. Struijk, T. P. DeMonte, M. L. G. Joy, and H. Stodkilde-Jorgensen, "Current density imaging and electrically induced skin burns under surface electrodes," *IEEE Trans. Biomed. Eng.*, vol. 52, no. 12, pp. 2024–2031, Dec. 2005, doi: 10.1109/TBME.2005.857677.

[3] A. Patriciu, K. Yoshida, T. P. DeMonte, and M. L. G. Joy, "Detecting skin burns induced by surface electrodes," in *2001 Conference Proceedings of the 23rd Annual International Conference of the IEEE Engineering in Medicine and Biology Society*, Oct. 2001, vol. 3, pp. 3129–3131 vol.3, doi: 10.1109/IEMBS.2001.1017466.

[4] Stecker MM, Patterson T, and Netherton BL, "Mechanisms of electrode induced injury. Part 1: theory," *Am. J. Electroneurodiagnostic Technol.*, vol. 46, no. 4, pp. 315–398, Dec. 2006.

[5] S. J. Dorgan and R. B. Reilly, "A model for human skin impedance during surface functional neuromuscular stimulation," *IEEE Trans. Rehabil. Eng.*, vol. 7, no. 3, pp. 341–348, Sep. 1999, doi: 10.1109/86.788470.

[6] X. Yu *et al.*, "An impedance detection circuit for applications in a portable biosensor system," in *2016 IEEE International Symposium on Circuits and Systems (ISCAS)*, May 2016, pp. 1518–1521, doi: 10.1109/ISCAS.2016.7527547.

[7] R. Kubendran, S. Lee, S. Mitra, and R. F. Yazicioglu, "Error Correction Algorithm for High Accuracy Bio-Impedance Measurement in Wearable Healthcare Applications," *IEEE Trans. Biomed. Circuits Syst.*, vol. 8, no. 2, pp. 196–205, Apr. 2014, doi: 10.1109/TBCAS.2014.2310895.

[8] A. van Boxtel, "Skin resistance during square-wave electrical pulses of 1 to 10 mA," *Med. Biol. Eng. Comput.*, vol. 15, no. 6, pp. 679–687, Nov. 1977, doi: 10.1007/BF02457927.

[9] "74HC86; 74HCT86 Quad 2-input EXCLUSIVE-OR gate," vol. 2017, p. 15, 2015.

[10] "Guidance Document for Powered Muscle Stimulator 510(k)s," p. 19.